Inorg. Chem. **2005**, *44*, 9197–9206

Copper(I) and -(II) Complexes of Neutral and Deprotonated *N*-(2,6-Diisopropylphenyl)-3-[bis(2-pyridylmethyl)amino]propanamide

Timothy E. Patten,* Christina Troeltzsch, and Marilyn M. Olmstead

Department of Chemistry, University of California at Davis, One Shields Avenue, Davis, California 95616-5292

Received April 12, 2005

As part of a study of atom-transfer radical polymerization (ATRP) catalysts, four new copper(I) and -(II) compounds of a new monoanionic, tripodal tetradentate ligand, *N*-(2,6-diisopropylphenyl)-3-[bis(2-pyridylmethyl)amino]propanamide (DIPMAP), were prepared. Ligand synthesis followed from the addition–elimination reaction of 2,6-diisopropylaniline with acryloyl chloride and then a Lewis acid catalyzed Michael addition of bis(2-pyridylmethyl)amine to this product. The ligand was complexed to CuCl to yield monomeric Cu(DIPMAP)Cl featuring an intramolecular hydrogen bond between the free amide hydrogen and the coordinated chloride ligand. Deprotonation of the amide hydrogen in Cu(DIPMAP)Cl using *n*-BuLi led to the incorporation of LiCl in the resulting product, $Li_2Cu_2(DIPMAP)_2Cl_2$. This complex exhibited an unusual dimeric structure, with the amine nitrogens of one ligand coordinated to a lithium ion, the amide oxygen of the same ligand bridging between the lithium ions, and the amidate nitrogen of that ligand coordinated to a CuCl unit that has a structure analogous to dihalocuprate ions. Deprotonation of Cu(DIPMAP)Cl using KO^{t}Bu yielded an alkali-metal chloride free product, $Cu_2(DIPMAP)_2$, that also exhibited a dimeric structure in which the three amine nitrogens of one ligand were coordinated to one Cu^I ion and the amidate nitrogen of the same ligand was coordinated to the other Cu^I ion. $Cu_2(DIPMAP)_2$ was effective in abstracting halogen atoms from organic halides, but in the attempted ATRP of *tert*-butyl acrylate, molecular weight versus conversion behavior reminiscent of a redox-initiated polymerization was observed. DIPMAP was coordinated to $CuBr_2$ to yield [Cu(DIPMAP)Br]Br with a square-pyramidal structure. The amide hydrogen in this complex could be deprotonated using KO^{t}Bu to form complex [DIPMAP]CuBr (**6**). Spectral characterization of complex **6** confirmed deprotonation of the ligand and that it most likely had an axially distorted trigonal-bipyramidal structure, although crystals suitable for X-ray analysis could not be obtained. Solution oxidation of $Cu_2(DIPMAP)_2$ using CBr_4 yielded a product, complex **4**, whose spectral signatures did not match those of complex **6**. The dimeric structure of $Cu_2(DIPMAP)_2$ might be a significant contributing factor to the slow rate of deactivation observed in atom-transfer reactions using $Cu_2(DIPMAP)_2$ as the catalyst.

Introduction

Copper (I) complexes have gained importance as catalysts for polymerizations and transformations that involve halogen atom-transfer chemistry. Atom-transfer radical addition (ATRA)[1−7] employs atom transfer from an organic halide to a transition-metal complex to generate and deactivate intermediate radicals that can undergo further addition reactions. The radical formed after the addition step is less stable than the initially formed radical, so after halogen atom abstraction from the higher oxidation state deactivator complex, the organic halide that is formed cannot react further with the metal catalyst. Atom transfer radical polymerization (ATRP)[8−12] is similar to ATRA but utilizes

* To whom correspondence should be addressed. E-mail: patten@chem.ucdavis.edu.

(1) Truce, W. E.; Goralski, C. T.; Christensen, L. W.; Bavry, R. H. *J. Org. Chem.* **1970**, *35*, 4217−4220.
(2) Minisci, F. *Acc. Chem. Res.* **1975**, *8*, 165−171.
(3) Tsuji, K.; Sato, K.; Nagashima, H. *Chem. Lett.* **1981**, 1169−1170.
(4) Bellus, D. *Pure Appl. Chem.* **1985**, *57*, 1827−1838.
(5) Curran, D. P. *Synthesis* **1988**, 489−513.
(6) Curran, D. P. In *Comprehensive Organic Synthesis*; Trost, B. M., Fleming, I., Eds.; Pergamon: Oxford, 1991; Vol. 4, p 715.
(7) Iqbal, J.; Bhatia, B.; Nayyar, N. K. *Chem. Rev.* **1994**, *94*, 519−564.
(8) Wang, J. S.; Matyjaszewski, K. *Macromolecules* **1995**, *28*, 7901−7910.

10.1021/ic0505697 CCC: $30.25
Published on Web 11/16/2005

organic halide polymer end groups that have similar reactivity before and after monomer addition, thus facilitating multiple addition processes and the growth of a polymer chain. The controlled nature of ATRA and ATRP (i.e., little or no radical−radical coupling or disproportionation) is derived from the persistent radical effect,[13−16] and with ATRP, polymers can be prepared with a high degree of synthetic control over the final molecular weight, molecular weight distributions, and end group structures.[17−20] When the higher oxidation state deactivator complex cannot react with the intermediate radical to form the dormant halide polymer chain end (or if the rate of such a reaction is too slow relative to the rate of radical propagation), the polymerization becomes a simple redox-initiated polymerization. Redox-initiated polymerizations display molecular weight behavior akin to free-radical polymerizations, and the mechanism of metal complex promoted radical formation can involve processes other than halogen atom transfer.[21]

Whether a given metal complex can promote ATRP versus a redox-initiated polymerization and the relative reactivity of the catalyst in ATRP depends very strongly on the nature of the ligands.[22] There are many combinations of polydentate amine-based ligands with copper(I) salts that are effective catalysts for ATRP and a few that promote only redox-initiated polymerization.[23,24] Changes in the ligand-sphere affect the polymerization kinetics and molecular weight control in ways that are often unexpected.[25−30] Thus, a better understanding of the inorganic chemistry side of copper(I) polymerization catalysts can be gained through knowledge about the structure, solution dynamics, and chemistry of the copper centers involved in the atom-transfer step.

The first barrier to developing ATRP catalyst systems that could be studied in solution was to reduce or eliminate the dynamic behavior observed for many of the ligand/copper(I) salt catalyst mixtures. Processes such as ligand dissociation, displacement, and exchange have all been observed and can be attributed to the d^{10} electronic structure of the copper(I) ion. Monoanionic, tripodal tetradentate ligand designs have been shown to be effective for preparing ATRP catalyst systems that exhibit simple solution structures that mirror their solid-state structures.[31] The stability of such complexes was achieved by maximizing the chelate effect and adding electrostatic attraction between the ligand and metal center. Additionally, the halide ligand is substituted by the anionic donor in the coordination sphere of the copper(I) center; thus, the complication of halide exchange between the alkyl halide and metal center is eliminated. In a prior example, the ligand's anionic donor was a sulfonamide group, so we sought to explore the different types of anionic donors, such as the amidato group[32−34] in this study, that might be applicable to the monoanionic, tripodal tetradentate ligand design.[35−38]

Experimental Section

Materials. Tetrahydrofuran (THF) was distilled from sodium benzophenone just prior to use. Chloroform, methylene chloride-d_2, and acetonitrile were stirred over P_2O_5, distilled, and degassed. Ethyl 2-bromopropionate was distilled from CaH_2 just prior to use. *tert*-Butyl acrylate, *p*-xylene, and triethylamine were stirred over CaH_2, distilled, and degassed. Methylene chloride was distilled from P_2O_5 just prior to use. Bis(2-methylpyridyl)amine was prepared by the condensation of (2-aminomethyl)pyridine and pyridine-2-carboxaldehyde over $MgSO_4$ followed by reduction of the imine intermediate using $NaBH_4$. Alumina gel for column chromatography was Acros aluminum oxide, activated and neutral (50−200 μm). Analytical thin-layer chromatography (TLC) was performed on commercial EM Science plates coated with aluminum oxide 60 F_{254}, neutral (0.2 mm thick). Unless stated otherwise, all materials were purchased from commercial sources and used without further purification. Reagents were handled under a nitrogen atmosphere using standard drybox and Schlenk techniques.

Characterization. ^{1}H NMR (400 MHz) and ^{13}C NMR (100 MHz) spectra were recorded on a Varian Inova 400 instrument. Chemical shifts, δ (ppm), were referenced to the residual proton signal or ^{13}C signal of the specified solvent. Number-averaged molecular weights (M_n), weight-averaged molecular weights (M_w), and molecular weight distributions (M_w/M_n) were determined using

(9) Wang, J. S.; Matyjaszewski, K. *J. Am. Chem. Soc.* **1995**, *117*, 5614−5615.
(10) Wang, J. S.; Matyjaszewski, K. *Macromolecules* **1995**, *28*, 7572−7573.
(11) Kato, M.; Kamigaito, M.; Sawamoto, M.; Higashimura, T. *Macromolecules* **1995**, *28*, 1721−1723.
(12) Ando, T.; Kato, M.; Kamigaito, M.; Sawamoto, M. *Macromolecules* **1996**, *29*, 1070−1072.
(13) Fischer, H. *J. Am. Chem. Soc.* **1986**, *108*, 3925−3927.
(14) Fischer, H. *Macromolecules* **1997**, *30*, 5666−5672.
(15) Daikh, B. E.; Finke, R. G. *J. Am. Chem. Soc.* **1992**, *114*, 2938−2943.
(16) Matyjaszewski, K.; Patten, T. E.; Xia, J. H. *J. Am. Chem. Soc.* **1997**, *119*, 674−680.
(17) Patten, T. E.; Xia, J. H.; Abernathy, T.; Matyjaszewski, K. *Science* **1996**, *272*, 866−868.
(18) Patten, T. E.; Matyjaszewski, K. *Adv. Mater.* **1998**, *10*, 1−15.
(19) Patten, T. E.; Matyjaszewski, K. *Acc. Chem. Res.* **1999**, *32*, 895−903.
(20) Kamigaito, M.; Ando, T.; Sawamoto, M. *Chem. Rev.* **2001**, *101*, 3689−3745.
(21) Odian, G. *Principles of Polymerization*; John Wiley and Sons: Hoboken, NJ, 2004.
(22) Qiu, J.; Matyjaszewski, K. *Acta Polym.* **1997**, *48*, 169−180.
(23) Haddleton, D. M.; Jasieczek, C. B.; Hannon, M. J.; Shooter, A. J. *Macromolecules* **1997**, *30*, 2190−2193.
(24) Xia, J. H.; Matyjaszewski, K. *Macromolecules* **1997**, *30*, 7697−7700.
(25) Haddleton, D. M.; Clark, A. J.; Crossman, M. C.; Duncalf, D. J.; Heming, A. M.; Morsley, S. R.; Shooter, A. J. *J. Chem. Soc., Chem. Commun.* **1997**, 1173−1174.
(26) Haddleton, D. M.; Heming, A. M.; Kukulj, D.; Duncalf, D. J.; Shooter, A. J. *Macromolecules* **1998**, *31*, 2016−2018.
(27) Matyjaszewski, K.; Nakagawa, Y.; Jasieczek, C. B. *Macromolecules* **1998**, *31*, 1535−1541.
(28) Percec, V.; Barboiu, B.; vanderSluis, M. *Macromolecules* **1998**, *31*, 4053−4056.
(29) Woodworth, B. E.; Metzner, Z.; Matyjaszewski, K. *Macromolecules* **1998**, *31*, 7999−8004.
(30) Wang, X.-S.; Lascelles, S. F.; Jackson, R. A.; Armes, S. P. *J. Chem. Soc., Chem. Commun.* **1999**, 1817−1818.
(31) Goodwin, J. M.; Olmstead, M. M.; Patten, T. E. *J. Am. Chem. Soc.* **2004**, *126*, 14352−14353.
(32) Ishikawa, Y.; Ito, S.; Nishino, S.; Ohba, S.; Nishida, Y. *Z. Naturforsch., C: J. Biosci.* **1998**, *53*, 378−382.
(33) Nishino, S.; Kunita, M.; Kani, Y.; Ohba, S.; Matsushima, H.; Tokii, T.; Nishida, Y. *Inorg. Chem. Commun.* **2000**, *3*, 145−148.
(34) Battacharya, S.; Snehalatha, K.; Kumar, V. P. *J. Org. Chem.* **2003**, *68*, 2741−2747.
(35) Inoue, Y.; Matyjaszewski, K. *Macromolecules* **2003**, *36*, 7432−7438.
(36) Inoue, Y.; Matyjaszewski, K. *Macromolecules* **2004**, *37*, 4014−4021.
(37) Olmstead, M. M.; Patten, T. E.; Troeltzsch, C. *Inorg. Chim. Acta* **2003**, *357* (2), 619−624.
(38) Olmstead, M. M.; Troeltzsch, C.; Patten, T. E. *Acta Crystallogr.* **2003**, *E59*, m502−m503.

Table 1. X-ray Refinement Data for DIPMAP Complexes

	complex **1**: (DIPMAP)$Cu^{I}Cl$·*n*-BuCN	complex **2**: $[Li(DIPMAP)Cu^{I}Cl]_2$·$2CH_3CN$	complex **3**: $[(DIPMAP)Cu^{I}]_2$	complex **5**: $[(DIPMAP)Cu^{II}Br]Br$·$0.175H_2O$
formula	$C_{31}H_{41}ClCuN_5O$	$C_{58}H_{72}Cl_2Cu_2Li_2N_{10}O_2$	$C_{54}H_{66}Cu_2N_8O_2$	$C_{27}H_{34.45}Br_2CuN_4O_{1.17}$
fw	598.68	1153.12	986.23	657.2
space group	*P*1	$P2_1/n$	*C*2/*c*	$P2_1/n$
a, Å	8.5385(6)	10.3087(8)	18.948(3)	22.460(3)
b, Å	9.6593(6)	22.191(2)	16.282(3)	8.8356(10)
c, Å	9.8370(7)	12.8290(9)	17.272(3)	29.944(3)
α, deg	103.197(1)	90	90	90
β, deg	106.646(1)	100.160(7)	112.815(4)	111.318(2)
γ, deg	94.001(1)	90	90	90
V, Å^3	748.80(9)	2888.69(18)	4911.7(15)	5535.9(11)
T, K	90(2)	91(2)	92(2)	91(2)
Z	1	2	4	8
ρ_{calc}, Mg cm^{-3}	1.328	1.326	1.334	1.577
μ(Mo Kα), mm^{-1}	0.851	0.879	0.916	3.704
range of transm factors	0.797−0.876	0.844−0.917	0.746−0.906	0.555−0.836
wR2[a] (all data)	0.0728	0.0982	0.1014	0.1026
R1[b] (obsd data)	0.0269	0.0391	0.0366	0.0493

[a] $wR2 = [\sum[w(F_o^2 - F_c^2)^2]/\sum[(wF_o^2)^2]]^{1/2}$; $w = 1/[\sigma^2(F_o^2) + (aP)^2 + bP]$, where $P = (F_o^2 + 2F_c^2)/3$. [b] $R1 = \sum||F_o| - |F_c||/\sum|F_o|$.

gel permeation chromatography (GPC) in THF at 30 °C. Three Polymer Standard Services columns (100 Å, 1000 Å, and linear) were connected in series to a Thermoseparation Products P-1000 isocratic pump, autosampler, column oven, and Knauer refractive index detector. Calibration was performed using polystyrene samples (Polymer Standard Services; $M_p = 400-1\,000\,000$; $M_w/M_n < 1.10$). Monomer conversion was determined using a Shimadzu GC 14-A gas chromatograph equipped with a J&W Scientific 30 M DB WAS Megabore column. Injector and detector temperatures were kept constant at 200 °C. The column temperature was held at 80 °C for the initial 2 min of the run followed by an increase to 150 °C with a heating rate of 10 °C/min. Compound elutions are reported in retention times, R_t (min), for these specific conditions. An internal standard, *p*-xylene, was used to quantify the amount of monomer present. UV−vis spectra were recorded on a Cary 17 with an Olis Conversion. Gas chromatography−mass spectrometry (GC−MS) experiments were reported on a Varian 3400 gas chromatograph with a Finnigan Mat ion trap detector. Elemental analyses were performed by Midwest Microlabs. Electron paramagnetic resonance (EPR) spectra were recorded at 100-kHz modulation and 10-G modulation amplitude on a Bruker ECS 106 spectrometer; unless otherwise noted, 0.80-mW incident power was used and resonance conditions were typically 9.69 GHz at 10 K.

X-ray Structure Determinations. Diffraction data were collected with a Bruker SMART 1000 diffractometer, graphite-monochromated Mo Kα radiation, and a nitrogen cold stream provided by a CRYO Industries apparatus. Corrections for absorption were applied using the program SADABS 2.03.[39] The structures were solved by direct methods (SHELXS-97)[40] and refined by full-matrix least-squares on F^2 (SHELXL-97).[40] All non-hydrogen atoms were refined with anisotropic thermal parameters. Hydrogen atoms on water molecules were located on a difference map and refined using distance restraints. Other hydrogen atoms were added by geometry and refined using a riding model. The maximum and minimum peaks in the final difference Fourier map for each structure can be found in the data tables located in the Supporting Information. Crystal data and refinement details for the complexes are shown in Table 1. For complex **5**, the structure contains two nearly identical molecules related by translation along the *a* direction. However, in the smaller unit cell ($a' = {}^1/_2a$), thermal ellipsoids are unreasonable. Because of the superlattice, intensity statistics appear to be worse than normal. There is a disordered atom, presumed to be from water, that is weakly coordinated to Cu1; no such atom is located near Cu2. The O1W atom occupancy refined to 0.32(2) and was fixed at 0.35 for future runs. No hydrogen was located for this water. Additional experimental information, including atomic positional parameters, is supplied in CIF format as described in the Supporting Information.

Synthesis of *N*-(2,6-Diisopropylphenyl)propenamide. A solution of 6.00 mL (31.8 mmol) of 2,6-diisopropylaniline and 4.50 mL (31.8 mmol) of triethylamine in 40 mL of dry CH_2Cl_2 was added dropwise to 2.64 mL (31.8 mmol) of acryloyl chloride in 40 mL of dry CH_2Cl_2 stirred in an ice bath. The reaction was stirred overnight. The solution was then washed with $NaHCO_3$ (50 mL), H_2O (50 mL), dilute HCl (50 mL), and H_2O (50 mL). The CH_2Cl_2 layer was dried over anhydrous Na_2SO_4, filtered, and concentrated. The resulting white powder was recrystallized from toluene, yielding 6.81 g (93%). Mp: 182−184 °C. ^{1}H NMR (300 MHz, DMSO-d_6): δ (ppm) 7.2 (m, 3H), 6.5 (dd, $J = 10.2$ Hz, 1H), 6.2 (d, $J = 15.3$ Hz, 1H), 5.7 (d, $J = 8.1$ Hz, 1H), 3.0 (p, $J = 6.9$ Hz, 2H), 1.1 (d, $J = 6.3$ Hz, 12H). ^{13}C NMR (75 MHz, DMSO-d_6): δ (ppm) 164.0, 154.7, 154.5, 145.7, 132.0, 121.0, 127.5, 126.0, 123.0, 28.1, 23.7, 23.3. IR (CH_2Cl_2): ν (cm^{-1}) 3415 (br), 3238 (br), 3052, 2966, 2870, 1662, 1625, 1525.

Synthesis of *N*-(2,6-Diisopropylphenyl)-3-[bis(2-pyridylmethyl)amino]propanamide (DIPMAP). To 50 mL of degassed toluene was added 3.17 g (13.7 mmol) of *N*-(2,6-diisopropylphenyl)-propenamide. Then 2.65 g (13.3 mmol) of bis(2-pyridylmethyl)-amide was added, along with 0.94 mL (7.32 mol) of BF_3·Et_2O. The reaction was stirred at reflux for 5 days. The solution was then extracted with 3 × 50 mL of 10% HCl. The acidic layers were combined, and the pH was adjusted to >9 with 10% NaOH. The resulting solution was then extracted with 4 × 100 mL of CH_2Cl_2. The organic layers were combined, dried over anhydrous Na_2SO_4, filtered, and concentrated. The crude product was purified using alumina column chromatography, eluted with 5% Et_3N in EtOAc. The fractions containing product (determined by TLC, $R_f = 0.603$) were combined and concentrated, and volatile materials were removed under vacuum, yielding 4.33 g (76%) of an orange gel. MS: *m*/*z* 430. ^{1}H NMR (400 MHz, CD_3CN): δ (ppm) 9.2 (s, 1H), 8.3 (d, $J = 3.9$ Hz, 2H), 7.7 (t, $J = 6$ Hz, 2H), 7.4 (d, $J = 7.8$ Hz, 2H), 7.2 (m, 6H), 3.9 (s, 4H), 3.1 (p, $J = 6.9$ Hz, 2H), 3.0 (t, $J =$

(39) Sheldrick, G. M. In *SADABS*, 2.03 ed.; Sheldrick, G. M., Ed.; Unviersity of Göttingen: Göttingen, Germany, 2000.
(40) Sheldrick, G. M. In *SHELXTL*, 5.10 ed.; Sheldrick, G. M., Ed.; Bruker Analytical X-ray Instuments, Inc.: Madison, WI, 1997.

6.3 Hz, 2H), 2.6 (t, $J = 6.3$ Hz, 2H), 1.1 (d, $J = 6.9$ Hz, 12H). ^{13}C NMR (100 MHz, DMSO-d_6): δ (ppm) 171, 159, 149, 146, 137, 133, 127, 123, 60, 51, 34, 29, 24.5, 24.0; IR (CH_2Cl_2): ν (cm^{-1}) 3239, 3187, 2964, 2868, 1670, 1590, 1526.

Synthesis of [*N*-(2,6-Diisopropylphenyl)-3-[bis(2-pyridylmethyl)amino]propanamide]copper(I) Chloride ([DIPMAP]-Cu^{I}Cl, 1). A solution of 1.09 g (2.54 mmol) of DIPMAP in 25 mL of dry CH_2CN was cannulated onto 0.252 g (2.55 mol) of CuCl. The mixture was stirred at reflux for 10 min and then allowed to cool slowly to 0 °C when yellow crystals formed. The solution was filtered, and all volatile materials were removed under vacuum, yielding 1.11 g (83%) of product. Crystals suitable for X-ray crystallography were grown by diffusion of hexane into a butyronitrile solution. Mp: 169−171°C. ^{1}H NMR (400 MHz, CD_3CN): δ (ppm) 8.7 (s, 1H), 8.5 (d, $J = 3.6$ Hz, 2H), 7.8 (d, $J = 7.5$ Hz, 2H), 7.4 (d, $J = 5.6$ Hz, 2H), 7.2 (t, $J = 7.2$ Hz, 2H), 7.1 (t, $J = 6.8$ Hz, 3H), 3.8 (s, 4H), 3.1 (d, $J = 7.2$ Hz, 2H), 7.1 (t, $J = 6.8$ Hz, 3H), 3.8 (s, 4H), 3.1 (d, $J = 7.2$ Hz, 2H), 3.0 (t, $J = 6.6$ Hz, 2H), 2.8 (d, $J = 7.2$ Hz, 2H), 1.0 (d, $J = 6.9$ Hz, 12H). ^{13}C NMR (150 MHz, CD_2Cl_2): δ (ppm) 172.5, 156.4, 149.8, 146.8, 137.2, 132.2, 127.9, 124.3, 123.9, 123.2, 59.9, 51.2, 38.0, 28.5, 23.9, 23.1; IR (CH_2Cl_2): ν (cm^{-1}) 3239, 3179, 2962, 2868, 1676, 1599, 1526. Anal. Calcd for $C_{31}H_{41}N_5OCuCl$: C, 62.19; H, 6.90; N, 11.70. Found: C, 61.7; H, 7.0; N, 11.2.

Synthesis of Lithium [*N*-(2,6-Diisopropylphenyl)-3-[bis(2-pyridylmethyl)amino]propanamidate]copper(I) Chloride (2). A solution of 0.600 g (1.13 mmol) of [DIPMAP]CuCl in 40 mL of dry THF was stirred at 0 °C while 0.810 mL (1.13 mmol) of *n*-BuLi was added dropwise. The solution was stirred overnight at room temperature. The resulting mixture was then filtered, and the filtrate was concentrated. The residue was recrystallized from dry CH_3CN, yielding 0.512 g (86%) of white crystals suitable for X-ray analysis. ^{1}H NMR (400 MHz, CD_3CN): δ (ppm) 9.14 (d, 2H), 8.36 (d, $J = 4.5$ Hz, 2H), 8.25 (s, 2H), 7.65 (t, $J = 6.5$ Hz, 4H), 7.2−6.8 (m, 12H), 4.49 (d, $J = 15$ Hz, 2H), 3.94 (d, $J = 3.9$ Hz, 4H), 3.82 (d, $J = 15.5$ Hz, 2H), 3.63 (d, $J = 15.5$ Hz, 2H), 2.95 (m, 2H), 2.85 (t, $J = 6.5$ Hz, 2H), 2.76 (d, $J = 5.5$ Hz, 2H), 2.60 (d, $J = 4.0$ Hz, 2H), 2.00 (d, $J = 4.0$ Hz, 2H), 1.87 (s, 4H), 1.03 (d, $J = 7.0$ Hz, 2H), 0.94−0.80 (m, 24H). ^{13}C NMR (150 MHz, CD_2Cl_2): δ (ppm) 177.5, 161.5, 160.6, 152.0, 151.7, 145.1, 145.0, 144.1, 140.3, 139.7, 126.8, 125.3, 124.2, 123.1, 63.4, 60.7, 54.5, 53.6, 38.1, 31.3, 30.1, 29.9, 25.9, 25.8, 25.6, 24.8. IR (CH_2Cl_2): ν (cm^{-1}) 2962, 2876, 1591, 1565.

Synthesis of [*N*-(2,6-Diisopropylphenyl)-3-[bis(2-pyridylmethyl)amino]propanamidate]copper ([DIPMAP]Cu, 3). A solution of 0.401 g (0.758 mmol) of [DIPMAP]CuCl in ~50 mL of dry CH_3CN was heated and then cannulated while hot onto 0.104 g (0.923 mmol) of potassium *tert*-butoxide (KO^{t}Bu). The reaction was stirred for 2 days and then hot filtered. The supernatant was cooled, and orange crystals that were suitable for X-ray analysis formed over several days. The solution was filtered, and the remaining volatile materials were removed under vacuum, yielding 0.320 g (81%) of product. ^{1}H NMR (400 MHz, CD_3CN): δ (ppm) 8.5 (d, $J = 4.4$ Hz, 1H), 8.4 (s, 2H), 7.8−7.0 (m, 29H), 5.3 (s, 5H), 4.0 (s, 6H), 3.5 (q, $J = 6.4$ Hz, 4H), 3.3 (q, $J = 7.2$ Hz, 4H), 3.1 (s, 3H), 3.0 (t, $J = 7.2$ Hz, 4H), 2.8 (d, $J = 8.4$ Hz, 1H), 2.6 (s, 2H), 1.2−0.7 (m, 36H). ^{13}C NMR (150 MHz, CD_2Cl_2): δ (ppm) 172.5, 156.4, 150.4, 149.2, 146.6, 137.7, 136.6, 132.2, 128.4, 127.4, 124.8, 124.5, 123.8, 123.4, 122.7, 60.8, 59.9, 59.0, 51.2, 38.0, 28.9, 28.0, 24.3, 23.5, 22.6. IR (CH_2Cl_2): ν (cm^{-1}) 2961, 2876, 1591, 1565. UV−vis: $\lambda_{max} = 360$ nm, $\epsilon = 996$ M^{-1} cm^{-1}. Anal. Calcd for $C_{54}H_{66}N_8O_2Cu_2$: C, 65.76; H, 6.75; N, 11.36. Found: C, 65.6; H, 6.8; N, 11.2.

Synthesis of [*N*-(2,6-Diisopropylphenyl)-3-[bis(2-pyridylmethyl)amino]propanamide]copper(II) Bromide ([DIPMAP]-Cu^{II}Br$_2$, 5). A solution of 0.987 g (2.30 mmol) of DIPMAP in 20 mL of dry CH_3CN was cannulated onto 0.533 g (2.38 mmol) of $CuBr_2$. The reaction was heated at reflux and then cooled. Volatile materials were removed by rotary evaporation, and the resulting blue-green solid was recrystallized from THF, yielding 0.934 g (62%) of crystals suitable for X-ray analysis. IR (CH_2Cl_2): ν (cm^{-1}) 3156, 2962, 2927, 2867, 1671, 1639, 1608, 1523. UV−vis: $\lambda_{max} = 816$ nm, $\epsilon = 425$ M^{-1} cm^{-1}. Anal. Calcd for $C_{27}H_{34}N_4OCuBr_2$: C, 49.59; H, 5.24; N, 8.57. Found: C, 47.1; H, 5.2; N, 8.0.

Synthesis of [*N*-(2,6-Diisopropylphenyl)-3-[bis(2-pyridylmethyl)amino]propanamidate]copper(II) Bromide ([DIPMAP]-CuBr, 6). A solution of 0.540 g (0.826 mmol) of [DIPMAP]$CuBr_2$ in 30 mL of dry CH_3CN was cannulated onto 0.101 g (0.902 mmol) of KO^{t}Bu. The reaction was stirred for 2 days and then filtered. Volatile materials were removed under vacuum. The resulting solid was recrystallized from dry THF, yielding 0.230 g (42%) of a green solid. IR (CH_3CN): ν (cm^{-1}) 2962, 2927, 2867, 1603, 1564. UV−vis: $\lambda_{max} = 786$ nm, $\epsilon = 80$ M^{-1} cm^{-1}.

Oxidation of [*N*-(2,6-Diisopropylphenyl)-3-[bis(2-pyridylmethyl)amino]propanamidate]copper(I) Using CBr_4, 4. To 2.0 mL of a 5.6×10^{-4} M solution of [DIPMAP]Cu in dry CH_3CN was added 3.7 mg (1.12×10^{-2} mmol) of CBr_4. The solution was stirred until the color turned green and the UV−vis spectrum showed no Cu^I present. IR (CH_3CN): ν (cm^{-1}) 2962, 2927, 2867, 1603, 1564. UV−vis: $\lambda_{max} = 786$ nm, $\epsilon = 80$ M^{-1} cm^{-1}.

Reaction of [*N*-(2,6-Diisopropylphenyl)-3-[bis(2-pyridylmethyl)amino]propanamidate]copper(I) with Benzyl Bromide in the Presence of TEMPO. A 4.0-mL sample of a 1.23×10^{-2} M solution of [DIPMAP]Cu in dry CH_3CN was diluted with 0.9 mL of dry CH_3CN. Then, 0.09 mL of a 1.09 M solution of TEMPO in dry CH_3CN was added, followed by the addition of 0.05 mL of benzyl bromide. At time intervals, 0.1-mL samples were taken and diluted with 1:100 bromobenzene/CH_2Cl_2 and injected into the GC−MS (benzyl bromide, $R_t = 5.02$; TEMPO, $R_t = 5.30$; benzyl-TEMPO derivative, $R_t = 7.33$).

Polymerization of *tert*-Butyl Acrylate. A 25-mL Schlenk flask was charged with an amount of Cu[DIPMAP] (see Table 3) and dry *p*-xylene. Dry *tert*-butyl acrylate and ethyl 2-bromopropionate were then added, and the flask was immersed in either a room-temperature water bath ($T = 25$ °C) or an ice bath ($T = 0$ °C). At time intervals, 0.5-mL samples were taken and added to 5 mL of THF. Concentrations were measured using GC, and molecular weights were determined by GPC. All GPC samples were passed through a short alumina column to remove copper from the samples.

Results and Discussion

The ligand in this study was *N*-(2,6-diisopropylphenyl)-3-[bis(2-pyridylmethyl)amino]propanamide (DIPMAP), which contained the basic structure of neutral tripodal tetradentate ligands that have been explored in ATRP studies and could be deprotonated to become monoanionic. DIPMAP was prepared in two steps. First, *N*-(2,6-diisopropylphenyl)-propenamide was prepared by the addition−elimination reaction of 2,6-diisopropylaniline with acryloyl chloride. Then, bis(2-pyridylmethyl)amine was added to the product via a Lewis acid catalyzed Michael addition (Scheme 1).

Scheme 1. Synthetic Route for the Preparation of DIPMAP

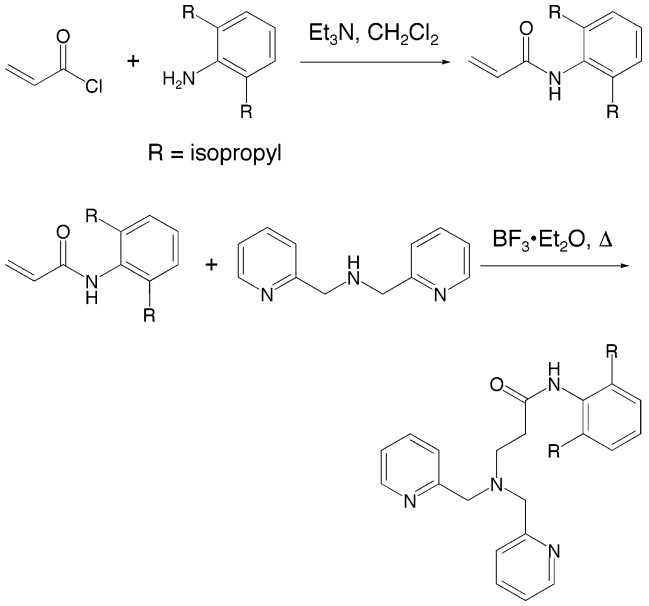

The complexation of DIPMAP with CuCl was accomplished when a CH_3CN solution of 1 equiv each of DIPMAP and CuCl was heated at reflux (eq 1). A yellow-orange

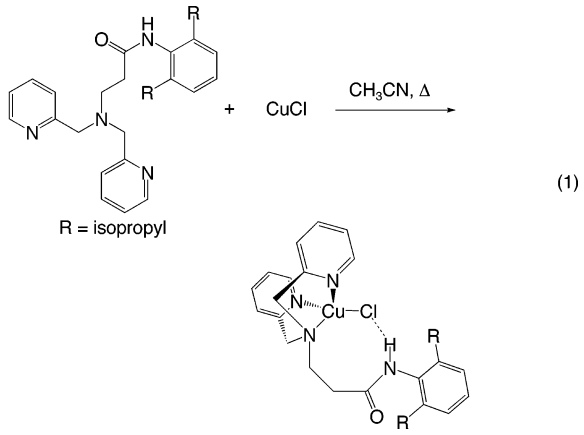

(1)

solution formed, and upon slow cooling, yellow crystals grew in 83% yield, complex **1**. Elemental analysis confirmed that the empirical formula of complex **1** was Cu[DIPMAP]Cl. Differences in the ^{1}H NMR chemical shifts of the pyridyl ring protons (8.5, 7.8, and 7.4 ppm) and the bridging methylene protons (3.1 and 2.9 ppm) in the product versus those of the free ligand (8.2, 7.7, and 7.4 ppm for the pyridyl ring protons and 2.8 and 2.6 ppm for the bridging methylene protons) also confirmed complex formation.

Crystals suitable for X-ray crystallography were grown from a butyronitrile/hexane solvent system. The molecular structure for complex **1** is shown in Figure 1, and the crystal data are contained in Table 1. The complex crystallized in the space group *P*1 with one molecule of butyronitrile. The geometry about the copper center is approximately tetrahedral with distortions due to the geometrical constraints of the ligand, and Table 2 shows key bond angle and distance data for the complex. The three bond angles containing a nitrogen atom, Cu1, and Cl1 are all greater than the ideal of 109.5°

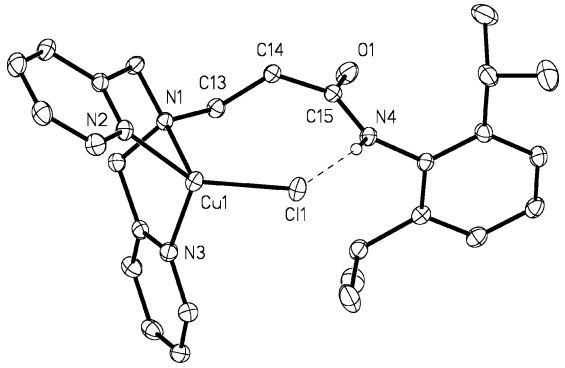

Figure 1. Molecular structure of complex **1**.

Table 2. Bond Lengths for DIPMAP Complexes

bond	complex **1**	complex **2**	complex **3**	complex **5**
amide C−N	1.357(2)	1.321(2)	1.336(3)	1.365(8),[a] 1.336(8)
amide C−O	1.232(2)	1.269(2)	1.252(2)	1.242(7),[a] 1.248(7)
3° amine−Cu	2.265(2)		2.234(2)	2.064(5),[a] 2.051(5)
pyridyl N−Cu	2.017(2)		2.063(2))	1.999(5),[a] 1.995(4)
pyridyl N−Cu	2.087(2)		2.141(2)	2.008(5),[a] 1.993(5)
Cu−amide N		1.875(2)	1.954(2)	
Cu−amide O				2.260(4),[a] 2.213(4)
H···Cl1	2.41			
H···Br2				2.54,[a] 2.54
Cu−Cl	2.252(2)	2.103(1)		

[a] Values for the complex with an additional coordinated water molecule.

(111°, 120°, and 130°). The two bond angles containing the central nitrogen donor atom, the copper center, and a pyridyl donor nitrogen atom are both 80°, while the bond angle containing the pyridyl donor nitrogen atoms and the copper center is 118°. All of these angles reflect the fact that the short methylene bridge between the central nitrogen atom and the pyridyl rings constrains the bite angle of the N1, N2 and N1, N3 pairs. The pyridyl C−C and C−N bond lengths as well as the N−Cu distances are within the range found for other pyridyl rings coordinated to copper(I) centers.[41−43] The X-ray structure also revealed a weak intramolecular hydrogen bond [N4···Cl1 distance of 3.2648(16) Å] between the amide proton and the chloride ligand bound to the copper center.[44]

The next step was to deprotonate the amide group in complex **1** and coordinate the anionic donor to the copper center via an intramolecular halogen metathesis reaction. A stoichiometric amount of *n*-butyllithium was added to a THF solution of complex **1** (eq 2). Colorless crystals were obtained, complex **2**, which was unexpected because pyridine/copper(I) complexes are colored as a result of metal-to-ligand charge-transfer absorptions, and the anticipated product would have this ligand set. Deprotonation of the amide group was confirmed by the absence of an amide proton signal at 8.7 ppm in the ^{1}H NMR spectrum and the absence of an N−H stretch at 3200 cm^{-1} in the IR spectrum.

(41) Levy, A. T.; Olmstead, M. M.; Patten, T. E. *Inorg. Chem.* **2000**, *39*, 1628−1634.
(42) Munakata, M.; Kitagawa, S.; Ashara, A.; Masuda, H. *Bull. Chem. Soc. Jpn.* **1987**, *1987*, 1927−1929.
(43) Dobson, J. F.; Green, B. E.; Healy, P. C.; Kennard, C. H. L.; Pakawatchai, C.; White, A. H. *Aust. J. Chem.* **1984**, *37*, 649−659.
(44) Emsley, J. *Chem. Soc. Rev.* **1980**, *9*, 91−124.

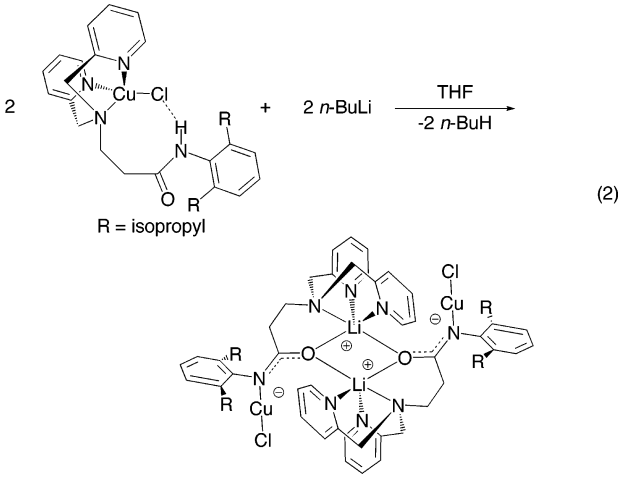

Crystals suitable for X-ray crystallography were obtained from CH_3CN. The molecular structure for complex **2** is shown in Figure 2, and the crystal data are contained in Table 1. The structure of complex **2** is that of a centrosymmetric dimer of Li[DIPMAP]CuCl consisting of a central ring of two lithium and two oxygen atoms flanked by two approximately linear N−Cu−Cl units. The asymmetric unit also contains a cocrystallized molecule of CH_3CN. The presence of four cations (two Li^+ and two Cu^+) and only two anions (two Cl^-) indicates that the amide group in complex **2** must be deprotonated in order to maintain overall charge neutrality. The lithium ions are five coordinate and are complexed to the three nitrogen donor atoms and the amidate oxygen atom of one ligand plus the amidate oxygen atom of the other ligand. A comparison of the amidate C−O [1.268(2) Å] and C−N [1.321(2) Å] bond distances in complex **2** (Table 2) with those of the amide in complex **1** [C−O = 1.230(2) Å and C−N = 1.357(2) Å] indicates a shorter C−N distance and a longer C−O distance in complex **2** relative to complex **1**. This is consistent with delocalization of the amidate negative charge onto both the nitrogen and oxygen atoms in complex **2**, as shown in eq 2. The presence of a negative charge on the amidate nitrogen makes it possible to form the linearly coordinated N1−Cu1−Cl1 cuprate structure. The Cu1−Cl1 distance of 2.1034(5) Å is consistent with those found in $CuCl_2^-$ ions (2.107 Å)[45] and is shorter than the Cu1−Cl1 distance found in complex **1** [2.2517(4) Å]. The N1−Cu1−C11 angle is 171.35(5)°, and the structure is bent away from the core of lithium and oxygen atoms. No specific interactions between the nearest lithium atom and the copper center at a distance of 3.260 Å away can be inferred because dihalocuprate ions are known to bend away from linear 180° coordination geometries depending upon the steric forces of crystal packing. The dihalocuprate-like structure of the copper(I) ion in complex **2** is also consistent with the observation that its crystals were colorless because the analogous $CuCl_2^-$ ion is also colorless ($CuBr_2^-$ is typically a very pale lilac or green color).[45]

The unwanted incorporation of LiCl into the product was most likely a consequence of its solubility in THF. Thus, KO^{t}Bu was used as the base in place of *n*-BuLi, because KCl is insoluble in relatively nonpolar and aprotic organic

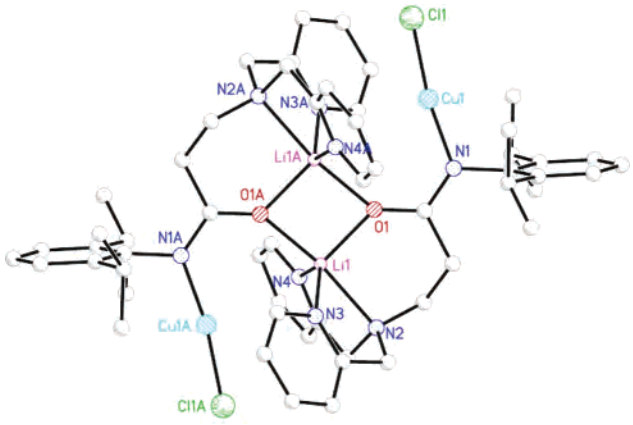

Figure 2. Molecular structure of complex **2**.

solvents such as THF or CH_3CN. A stoichiometric amount of KO^{t}Bu was added to [DPPMAP]Cu^{I}Cl in CH_3CN, and the solution was stirred (eq 3). After removal of a precipitate

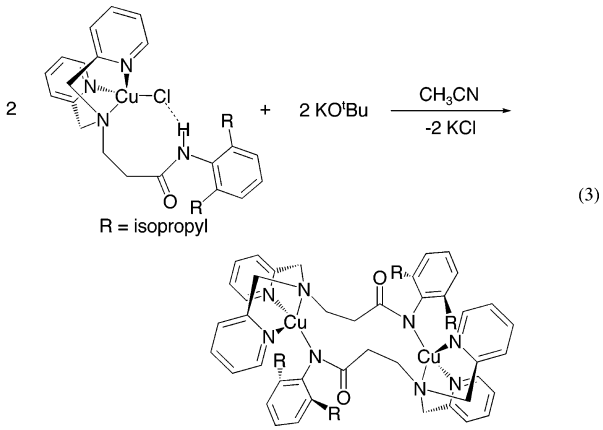

by filtration, the filtrate was set aside and orange crystals formed, complex **3**. Elemental analysis indicated that complex **3** had the empirical formula Cu(DIPMAP). The IR spectrum of this complex did not show a broad signal at 3200 cm^{-1} expected for amides, and the signal for the C=O stretch at 1676 cm^{-1} seen for complex **1** was replaced by a signal at 1565 cm^{-1}, consistent O−C−N stretching frequencies for metal-coordinated amidates.[46] The ^{1}H NMR spectrum of complex **1** exhibited two sets of signals, and it appeared as if the spectrum were doubled, consistent with two similar complexes or a monomer/dimer equilibrium mixture.

The crystals formed from the filtrate were suitable for X-ray analysis. The molecular structure of complex **3** is shown in Figure 3, and the crystal data are contained in Table 1. The structure is a centrosymmetric dimer with each half unit consisting of the pyridyl and central amine donor of one ligand coordinated to one copper center with the amidate nitrogen of the same ligand coordinated to the second copper center. The geometry of the copper centers is distorted tetrahedral. The N−Cu−N angles from the central donor atom, N2, are 79.61(7)°, 80.99(7)°, and 140.04(7)° (Table

(45) Nilsson, M. *Acta Chem. Scand. B* **1982**, *36*, 125−126.
(46) Patterson, R. E.; Gordon-Wylie, S. W.; Woomer, C. G.; Norman, R. G.; Weintraub, S. T.; Horwitz, C. P.; Collins, T. J. *Inorg. Chem.* **1998**, *37*, 4748−4750.

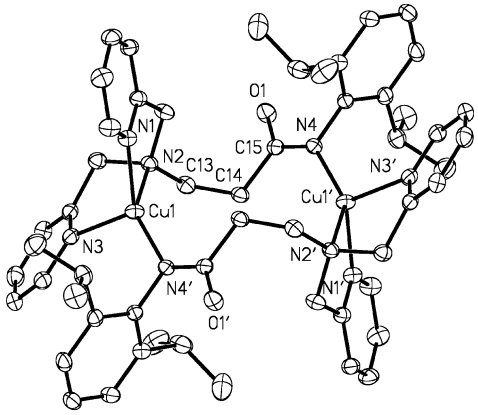

Figure 3. Molecular structure of complex **3**.

2), indicating that the bite angles between the pyridyl nitrogen atoms and the central nitrogen atom are too small to accommodate tetrahedral 109.5° geometry. Dimer formation is most likely driven by steric strain that would be present in the hypothetical monomeric complex: the three-carbon bridge between the central donor nitrogen and the amidate nitrogen is too short to accommodate the 140° corresponding N−Cu−N angle observed in the dimer. The monomeric species most likely adopts a severely distorted tetrahedral geometry. Inspection of the coordination geometry and bite angles available to DIPMAP indicates that the copper atom in such a monomeric complex would be very close to the tetrahedral face of the three pendant donor atoms, N1, N3, and N4. Formation of a dimer, as in complex **3**, would effectively release this strain. A solution equilibrium between the monomer and dimer would be consistent with the doubling of signals in the ^{1}H NMR spectrum. Complex **3**, the dimer, may have preferentially crystallized from the solution. The pyridyl C−C and C−N bond lengths as well as the N−Cu distances are within the range found for other pyridyl rings coordinated to copper(I) centers.[41−43] A comparison of the bond lengths of C15−N4 [1.337(3) Å] and C15−O1 [1.252(3) Å] with those of complexes **1** and **2** shows that these distances are between those found for complexes **1** and **2**. Thus, it is reasonable to conclude that while the negative charge of the amidate group is delocalized, more of the charge is localized on the nitrogen atom next to the positively charged copper center.

The reaction of complex **3** with benzyl bromide was studied to see if the compound would promote halogen atom transfer. Complex **3** was dissolved in dry CH_3CN, and then

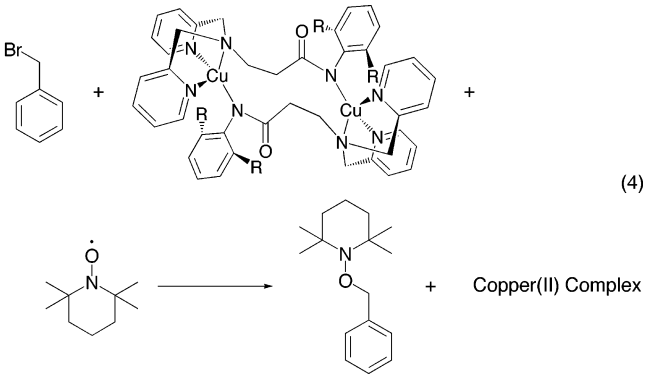

Table 3. Data for the Polymerization of *tert*-Butyl Acrylate in *p*-Xylene with a [DIPMAP]Cu^I Catalyst System

[M] (M)	[M]/ [I]	[I]/ [Cu]	% yield	M_n	M_n(theor)	M_w/M_n	temp (°C)	time (min)
5.15	91	3.65	85	1.8×10^{-4}	9.9×10^{-3}	2.05	25	10
3.38	88	11.05	46	5.4×10^{-4}	5.2×10^{-3}	1.42	25	91
2.55	84	4.26	50	1.8×10^{-4}	5.4×10^{-3}	1.39	25	108

a 10-fold excess of TEMPO and an equimolar amount of benzyl bromide were added (eq 4). Over time, the components of the solution were monitored using GC−MS, and the benzyl bromide (R_t = 5.02) was converted to the benzyl-TEMPO adduct (R_t = 7.33). This transformation demonstrated that complex **3** was capable of abstracting halogen atoms from certain organic halides to generate radicals.

Complex **3** was then examined as a potential ATRP catalyst (eq 5 and Table 3). A polymerization of *tert*-butyl

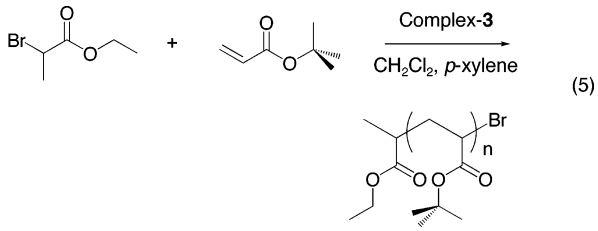

acrylate initiated using ethyl 2-bromopropionate was attempted using an initiator to complex **3** ratio of 4:1 and a monomer to initiator ratio of 90:1. The resulting polymerization was extremely rapid, reaching 85% conversion after just 10 min, and the molecular weight control was poor, as shown by the molecular weight distribution (M_w/M_n) of 2.05. The molecular weight versus conversion plot deviated from the linear correspondence normally observed for controlled/living polymerizations. Reducing the polymerization temperature to 0 °C slowed the rate of polymerization such that minimal conversion was observed over the course of a few hours. Increasing the ratio of initiator to complex **3** from 4:1 to 11:1 while holding the monomer to initiator ratio constant, produced a more narrow molecular weight distribution. Reducing the monomer concentration by half while holding the monomer to initiator ratio and the initiator to complex **3** ratio constant led to the best molecular weight distribution, but the molecular weight versus conversion plots still did not show a linear correlation and the molecular weights were too high by factors ranging from 2 to 9. This polymerization behavior strongly indicated that the deactivation of the organic radical, by reabstraction of a halogen atom from the copper(II) complex, was too slow relative to the rate of propagation. The polymerization displayed more characteristics of a redox initiated polymerization than a controlled polymerization. The polymerization of styrene was attempted, but at the temperatures necessary for this reaction, complex **3** underwent decomposition to an insoluble brown solid.

To gain a better understanding about the radical deactivation process for this ATRP system, we attempted to isolate and identify the copper(II) complex formed after atom

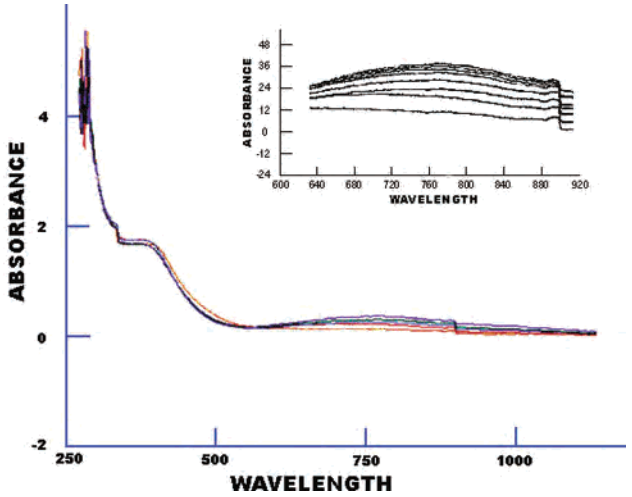

Figure 4. Overlay of UV−vis spectra at different times of the reaction between complex **3** and CBr_4 plus registered plot of the expanded region of the long-wavelength portion of the spectra.

transfer. Carbon tetrabromide, an efficient halogen atom-transfer oxidizing agent, was added to a solution of complex **3** (eq 6), and the reaction was monitored using UV−vis

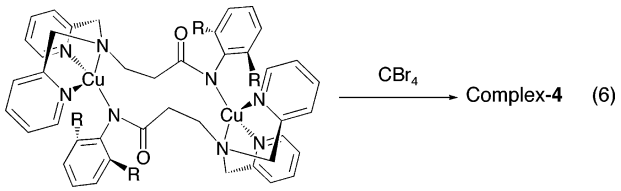

(6)

spectroscopy (Figure 4). A decrease in the intensity of the ligand-to-metal charge-transfer band at 360 nm was observed along with the growth of a d−d transition band of a new copper(II) species, complex **4**, at 786 nm ($\epsilon = 80$ L mol^{-1} cm^{-1}). An isosbestic point was observed in overlay spectra, indicating that complex **3** was converted directly into complex **4**. Unfortunately, it was not possible to isolate complex **4** cleanly upon repeated attempts.

Hence, we tried to prepare and characterize a copper(II) complex from deprotonated DIPMAP and $CuBr_2$ and then match its spectroscopic signatures to those of complex **4**. One equivalent of DIPMAP was added to $CuBr_2$ in CH_3CN, and the solution was heated at reflux (eq 7). Blue-green

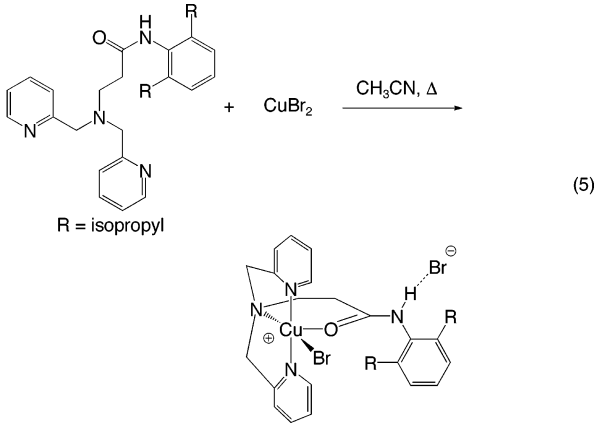

(5)

crystals formed almost immediately in good yield, which

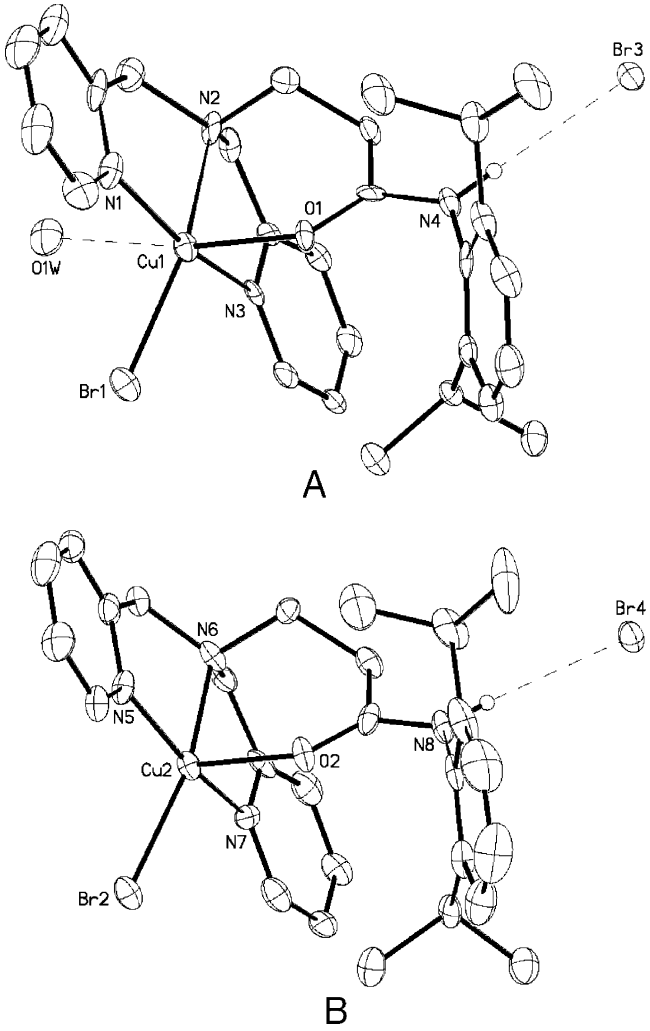

Figure 5. Molecular structure of complex **5** showing (A) the molecule with a coordinated water and (B) the molecule with a vacant sixth coordination site.

were recovered and recrystallized from THF, complex **5**. Crystals suitable for X-ray analysis were obtained from this process. Crystal data are contained in Table 1. There are two complexes in the asymmetric unit, shown as A and B in Figure 5. In molecule A, the pyridyl nitrogens, the amine nitrogen (N2), and Br1 are in the square plane, and the amide oxygen (O1) is in the axial position. An additional disordered water oxygen (O1W) is at 0.35 occupancy and is trans to the axial amide oxygen; it exhibits a long Cu−O distance of 2.695(12) Å (Table 2). Molecule B has no atom in the sixth coordination site. There are minor, yet significant, differences between the two molecules. The C−O and C−N bond distances in the amide group are consistent with those found in complex **1**. About the copper centers, the N−Cu−N bond angles range from 81.2° to 82.8°, which reflects the chelate bite angle of the ligand. Correspondingly, the N−Cu−Br bond angles are a bit greater than 90°: 96.1−98.3°. The copper centers are displaced outward from the square plane, which is reflected in the O−Cu−N and O−Cu−Br bond angles being slightly greater than 90°: 91.8−101.5°. The copper−pyridine N bond lengths range from 1.993(5) to 2.008(5) Å, and the copper−tertiary amine

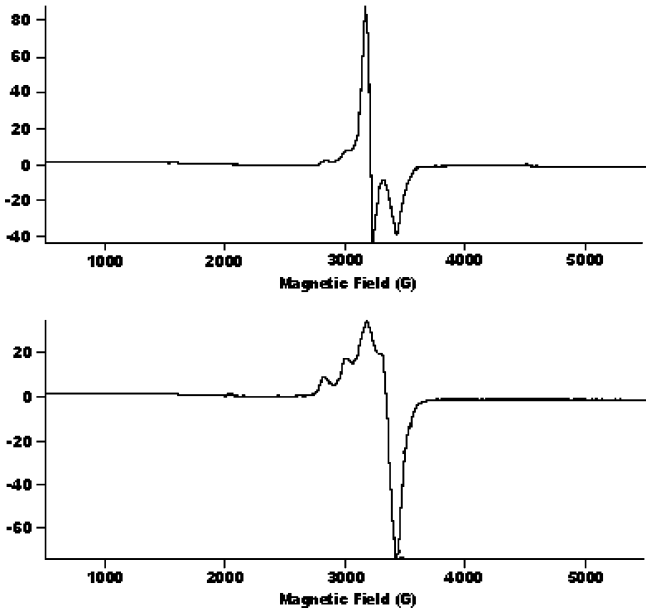

Figure 6. EPR spectra of complexes **4** (top) and **6** (bottom).

N bond lengths are 2.064(5) and 2.051(5) Å, which are consistent with the values found in complexes similar to those of Cu^{II}. The Cu−Br bond distances are also similar to those found in Cu^{II} complexes. The copper−amide oxygen bond distances show some variation, depending upon the presence of the additional water ligand: Cu2−O2, 2.213(4) Å, in the water-free complex was slightly shorter than Cu1−O1, 2.260(4) Å, in the complex with the coordinated water. This small difference is most likely due to the trans influence of the water ligand. The free bromide anion is hydrogen bonded to the amide hydrogen, with N−Br distances of 3.390(5) (N4−Br3) and 3.328(5) Å (N8−Br4).

A stoichiometric amount of KO^tBu was added to complex **5** in CH_3CN (eq 8). After removal of a precipitate by

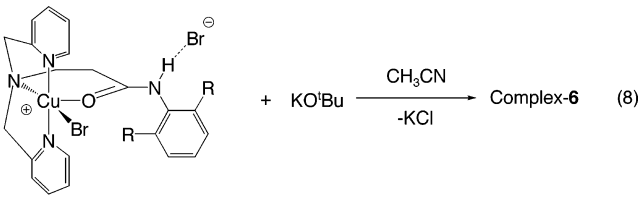

R = isopropyl

filtration, the resulting solid was recrystallized from THF, complex **6**. Repeated attempts to grow crystals of this complex failed to yield crystals suitable for X-ray analysis. Deprotonation of the amide hydrogen was confirmed by the absence of a signal at 3200 cm^{-1} in the IR spectrum. The UV−vis spectrum of complex **6** showed a d−d transition at 786 nm ($\epsilon = 80$ L mol^{-1} cm^{-1}). Considering the similarities of the UV−vis spectra, we then compared the EPR spectra of complexes **4** and **6**. As seen in Figure 6, both complexes had similar g values ($g_{||} = 2.2$ and $g_{\perp} = 2.0$), analogous to those of other copper(II) complexes with comparable, noncentrosymmetric ligand spheres.[47,48] However, the spectra of the two complexes were noticeably different in appearance. The spectrum for complex **6** exhibited hyperfine coupling to the Cu nucleus with $A_{||} = 150$ G, similar to other examples of axially distorted trigonal-bipyramidal N_4Br-Cu^{II} complexes.[31] The spectrum for complex **4** appears quite different from that of complex **6**, and barring further characterization, we can only tentatively postulate that the structure of complex **4** is not distorted trigonal-bipyramidal. The structure of complex **3** is dimeric, so it is reasonable to assume that after atom transfer the resulting complex would be a mixed Cu^I-Cu^{II} dimeric species or quite possibly that significant ligand-sphere reorganization occurs to yield separate copper(I) and (II) complexes. Both possibilities could account for the slow rate of deactivation observed in the ATRP of acrylates using complex **3**.

Conclusions

A new monoanionic, tripodal tetradentate ligand, *N*-(2,6-diisopropylphenyl)-3-[bis(2-pyridylmethyl)amino]propanamide (DIPMAP), was prepared by the addition−elimination reaction of 2,6-diisopropylaniline with acryloyl chloride and then a Lewis acid catalyzed Michael addition of bis(2-pyridylmethyl)amine to this product. The ligand was complexed to CuCl to yield a monomeric complex with a N_3Cl donor set, complex **1**, featuring an intramolecular hydrogen bond between the free amide hydrogen and the coordinated chloride ligand. Deprotonation of the amide hydrogen in complex **1** using *n*-BuLi led to the incorporation of LiCl in the resulting product, complex **2**. Complex **2** exhibited an unusual dimeric structure with the amine nitrogens of one ligand coordinated to a lithium ion, the amide oxygen bridging between the lithium ions, and the amide nitrogen coordinated to a CuCl unit with a structure analogous to dihalocuprate ions. Deprotonation of complex **1** using KO^tBu yielded an alkali-metal chloride free product, complex **3**, that also exhibited a dimeric structure in which the three amine nitrogens of one ligand were coordinated to one Cu^I ion and the amidate nitrogen of the same ligand was coordinated to the other Cu^I ion. Complex **3** was effective in abstracting halogen atoms from organic halides, but in the attempted ATRP of *tert*-butyl acrylate, the complex only showed polymerization behavior reminiscent of a redox-initiated polymerization. DIPMAP was coordinated to $CuBr_2$ to yield a N_3OBr donor set with a square-pyramidal structure, complex **5**. The amide hydrogen in complex **5** could be deprotonated using KO^tBu to form complex **6**. Spectral characterization of complex **6** indicated that deprotonation had occurred and that it most likely had an axially distorted trigonal-bipyramidal structure, although crystals suitable for X-ray analysis could not be obtained so confirmation of this conclusion was not possible. Solution oxidation of complex **3** using CBr_4 yielded a product, complex **4**, whose spectral signatures did not match those of complex **6**,

(47) Peisach, J.; Mims, W. B. *Chem. Phys. Lett.* **1976**, *37*, 307−310.

(48) Kurosaki, H.; Hayashi, K.; Ishikawa, Y.; Goto, M.; Inada, K.; Taniguchi, I.; Shionoya, M.; Kimura, E. *Inorg. Chem.* **1999**, *38*, 2824−2832.

indicating that the dimeric structure of complex **3** might be a significant factor in the slow rate of deactivation observed in atom-transfer reactions using complex **3** as the catalyst.

Acknowledgment. We thank the ACS Petroleum Research Fund (35150-AC7) for support of this research. We also thank the research group of Dr. David Britt (UCD) for their assistance with EPR.

Supporting Information Available: Crystallographic data for complexes **1**−**3** and **5**. This material is available free of charge via the Internet at http://pubs.acs.org.

IC0505697